

Selective electron beam melting of TiAl alloy: Microstructure evolution, phase transformation and microhardness

Yuyong Chen^{a,b}, Hangyu Yue^{a,b,*}, Xiaopeng Wang^{a,b}, Shulong Xiao^{a,b}, Fantao Kong^{a,b}, Xiangkui Cheng^c, Hui Peng^d

^a State Key Laboratory of Advanced Welding and Joining, Harbin Institute of Technology, Harbin 150001, China

^b School of Materials Science and Engineering, Harbin Institute of Technology, Harbin 150001, China

^c Panzhihua University, Panzhihua 617000, China

^d School of Materials Science and Engineering, Bethang University, Beijing 100191, China

ARTICLE INFO

Keywords:

Selective electron beam melting
TiAl alloy
Phase transformation
Microstructure evolution
Microhardness

ABSTRACT

In this research, a Ti-47Al-2Cr-2Nb alloy was fabricated by selective electron beam melting (SEBM). The microstructures at different heights of SEBM-produced TiAl alloy sample and their contribution to microhardness were investigated. The results revealed that the last deposited layers displayed near lamellar structure with fine α_2 lamellae. Lamellar colonies degraded at the height of 19 mm of the as-built sample, accompanied with the α_2 lamellae decomposition and B2 precipitation along primary α_2 lamellae. Meanwhile, equiaxed γ and blocky B2 phase dispersed on the colony boundaries. Lamellar colonies further degraded and colony boundaries further coarsen at the heights of 15 mm and 5 mm due to the in-situ heat treatment during SEBM process. Three kinds of phase transformations could be observed during SEBM process, which were $\alpha_2 \rightarrow \gamma$, $\alpha_2 \rightarrow B2$ and $\alpha_2 + \gamma \rightarrow B2$. The microhardness exhibited slight fluctuation as the building height increased from 3 mm to 19 mm, and the microhardness rapidly increased with the building height increasing from 19 mm to 20 mm. Eventually, the mechanism of microstructure evolution during SEBM process was discussed in detail.

1. Introduction

TiAl alloy, due to its low density, excellent specific strength and outstanding resistance against oxidation, has been widely used in the field of automotive and aerospace [1–3]. However, because of its intermetallic nature and inherent brittleness, the physical metallurgy of TiAl alloy is very demanding and further application is limited [4]. Fortunately, additive manufacturing (AM), as an attractive manufacturing technique, can fabricate complex parts from a computer aided design (CAD) model directly. Selective electron beam melting (SEBM) is an AM process and adopts a high-energy electron beam as heat source and selectively melt powder bed under a high vacuum, which can maintain the preheat temperature above 1000° [5, 6]. Therefore, SEBM is a preferential selection to manufacture TiAl alloy parts to avoid pickup of impurities and generation of cracks during SEBM process on account of TiAl's high affinity for oxygen and inherent brittleness.

Because of the wide application prospect in aerospace industry, TiAl alloy components fabricated by SEBM have attracted much attention and been investigated in recent years. Murr et al. [7] characterized the TiAl alloy components fabricated by SEBM and found the

microstructure exhibited an equiaxed γ -TiAl grain structure with a lamellar colony structure. Schwerdtfeger and Korner [8] researched the microstructure of SEBM-fabricated TiAl alloy, and observed that the last deposited layer displayed epitaxial growth columnar crystal. The microstructure consisted mainly of mixture of left elongated grains and equiaxed colonies below the last layer. Additionally, when the last layer was rescanned, the top of columnar crystal became fine grains. Therefore, the heat input had a significant effect on microstructure. It was well known that heat input during SEBM fabrication was complicated and highly dynamic, because the solidified microstructure underwent fast heating and cooling during scanning adjacent tracks and upper layers. The preheat temperature usually maintained above 1000 °C to avoid the accumulation of residual stress and generation of cracks, which can be identified as long-term annealing treatment during the entire SEBM fabrication. It was thus easy to imagine that phase transformation and microstructure evolution occurred during SEBM process. The microstructure evolution has been found and reported in SEBM-produced Ti alloys. Murr et al. [9] documented that there existed differences on a build height in microstructure and the corresponding hardness in EBM-built Ti-6Al-4V alloy samples. Tan et al. [10]

* Corresponding author at: State Key Laboratory of Advanced Welding and Joining, Harbin Institute of Technology, Harbin 150001, China.
E-mail address: yuehangyuyhy@163.com (H. Yue).

<https://doi.org/10.1016/j.matchar.2018.06.027>

Received 29 March 2018; Received in revised form 9 June 2018; Accepted 22 June 2018

Available online 23 June 2018

1044-5803/ © 2018 Elsevier Inc. All rights reserved.

investigated the dependence of microstructure of SEBM-fabricated Ti alloys on the building height and found that the prior β grain width and β interspacing increased with the build height due to the decreasing cooling rate.

Because of the complex thermal history, the microstructure was often varying spatially inside of a sample. It was significant to understand how the microstructure evolved during SEBM fabrication of TiAl alloys. However, there was a dearth of information in the literature on the microstructure difference at different heights of TiAl alloy sample manufactured by SEBM, and the processes of phase transformation and microstructure evolution were not clear although several investigations on TiAl alloy fabricated by SEBM were reported [11–13]. Therefore, for the purpose of the present paper, the focus was the microstructure variation of TiAl alloy samples fabricated by SEBM at different heights and their contribution to microhardness. Furthermore, microstructure evolution during SEBM process was discussed in detail.

2. Experimental

SEBM experiments were conducted on Arcam A2 equipment under a vacuum of 1×10^{-3} mBar. The zig-zag pattern with a 90° rotation between adjacent two layers was adopted to manufacture cubic samples with the dimension of $20 \times 20 \times 20 \text{ mm}^3$, as shown in Fig. 1. The preheating temperature was set as 1060°C , and once the substrate temperature reached to 1060°C , selective melting started. Specific processing parameters are shown in Table 1. Finally, near fully dense (porosity < 1%) and crack-free TiAl alloy sample was fabricated by SEBM in this work. The initial 1 mm to 2 mm distance from the substrate of as-built sample was not considered.

Pre-alloyed powders of Ti-47Al-2Cr-2Nb with particle diameters ranging from $45 \mu\text{m}$ to $200 \mu\text{m}$, were used to manufacture the TiAl alloy samples by SEBM. The specimens for microstructure observation were cut from the built sample by electric discharging. Four different locations at the heights of 20 mm, 19 mm, 15 mm and 5 mm were selected and the corresponding microstructures were examined from the horizontal cross-section parallel to the top surface, which were marked by S1, S2, S3 and S4, respectively, as can be seen from Fig. 1. Scanning electron microscopy (SEM), electron backscattered diffraction (EBSD) and transmission electron microscopy (TEM) were used to characterize the microstructure of SEBM-produced TiAl alloy samples. SEM specimens were grinded and electro-polished in a solution of 10% perchloric acid, 30% butanol and 60% methanol by volume at -45°C . EBSD samples were the same as that of SEM. TEM specimens were manufactured by twin-jet electro-polishing with the same electrolyte as that of SEM. X-ray diffraction (XRD) was used to determine the phase compositions and the diffraction angle of 2θ ranged from 20° to 90° with a scanning rate of $10^\circ/\text{min}$ and a step size of 0.02° .

Inductively coupled plasma (ICP) was used to identify the chemical compositions of pre-alloyed powders. Meanwhile, the chemical

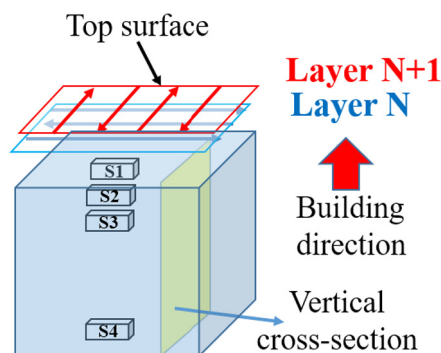


Fig. 1. Scanning strategy of SEBM process and the location of observed microstructure at different heights.

Table 1

Processing parameters of SEBM-fabricated TiAl alloy samples. I is the beam current, v is the scanning speed, d is the layer thickness and h is the hatch space.

Parameters	$I(\text{mA})$	$v(\text{mm/s})$	$d(\mu\text{m})$	$h(\mu\text{m})$
Value	7.6	2100	90	100

Table 2

Chemical compositions of the pre-alloyed powder and as-fabricated sample.

Sample	Elemental chemical composition			
	Ti[at.%]	Al[at.%]	Cr[at.%]	Nb[at.%]
Powder	48.85	47.02	1.98	1.94
As-built	50.77	45.38	1.95	1.90

compositions of as-built sample were determined using X-Ray Fluorescence (XRF) spectroscopy. The results are displayed in Table 2 and it is worth mentioning that the actual Al content decreased to 45.38 at. % because of Al evaporation during SEBM process.

The microhardness was measured by using a digital microhardness tester under a load of 500 g for 10s along the building direction in the vertical cross section. The microhardness was measured from 3 mm to 20 mm. The hardness values were determined by 3 measurements at the same height of as-built sample.

3. Results

3.1. Phase Composition

XRD is used to determine the phase compositions at different heights of the SEBM-produced TiAl alloy sample and the results are shown in Fig. 2. As can be seen from Fig. 2, the strongest diffraction peak was located in 38.96° for samples S1, S2 and S4 and 44.37° for sample S3, which belonged to (111) γ and (002) γ , respectively, and thus γ was identified as the matrix phase. The peak intensities at 26.11° and 28.16° corresponding to the (101) α_2 and (100) B2 in sample S3 could be obviously detected and were the strongest in the four samples but almost cannot be seen in sample S1. The peak intensities of (300) α_2 and (200) B2 located at 54.85° and 58.24° in sample S3 were the strongest but those in sample 1 were the weakest. The results revealed that the B2 and α_2 contents were the most in sample S3 and were the least in sample S1.

3.2. Microstructure

EBSD is introduced and conducted on SEBM-produced TiAl alloy sample to characterize the microstructure and quantify the phase compositions. Fig. 3 illustrates the microstructures of transverse cross-section (parallel to top surface) at different heights of SEBM-produced Ti-47Al-2Cr-2Nb alloy sample. As revealed in Fig. 3(a), the microstructure in the last deposited layer (sample S1) featured near lamellar structure, with a small number of equiaxed γ grains and blocky B2 particles dotting on colony boundaries, which was considered as the starting microstructure. The volume fraction of γ phase was overwhelming and few α_2 and B2 phases were visible, whose compositions were 99.4%, 0.06% and 0.54%, respectively. As the building height decreased to 19 mm, it could be observed that intermittently ellipsoid-shape B2 particles with a high aspect ratio precipitated along the primary α_2 lamellae within lamellar colonies. Additionally, coarsening of colony boundaries occurred compared with that of the microstructure in sample S1, accompanied with precipitations of equiaxed γ phase and blocky B2 particles. The contents of α_2 and B2 phases increased, whose compositions accounted for 1.69% and 6.06%, and the concentration of γ phase decreased to 92.25%, as shown in Fig. 3(b). Fig. 3(c) shows the

Download English Version:

<https://daneshyari.com/en/article/7969139>

Download Persian Version:

<https://daneshyari.com/article/7969139>

[Daneshyari.com](https://daneshyari.com)